

Dynamics of vibronically excited fluorene–Ar_n (*n*=4, 5) clusters

Jonathan D. Pitts and J. L. Knee

Department of Chemistry, Wesleyan University, Middletown, Connecticut 06459

(Received 9 February 1998; accepted 10 March 1998)

The fluorene–Ar₄ cluster has been shown to exhibit two distinct isomers when formed in a molecular beam. Resonance enhanced multiphoton ionization and mass analyzed threshold ionization experiments have been performed to investigate the structural properties, energetics and dynamics of these clusters when excited to vibronic bands in the *S*₁ electronic state, with a specific interest in measuring isomer interconversion. At 208 cm⁻¹ excess energy in the *S*₁ isomer interconversion is not observed in the Ar₄ cluster. Dissociation of the Ar₅ cluster from the 722 cm⁻¹ band is shown to produce both Ar₄ isomers. © 1998 American Institute of Physics.
[S0021-9606(98)00523-6]

I. INTRODUCTION

Aromatic-rare gas clusters have been the focus of intense study in recent years.^{1–26} They provide particularly simple model systems for studying gas phase cluster properties including studies of cluster structure, mapping of intermolecular potentials, and cluster dynamics. While clusters formed with molecular binding partners potentially have a richer chemistry, there are often complications in the spectroscopy which make interpretation more difficult. In the present study the relatively simple systems fluorene–Ar₄ and fluorene–Ar₅ are studied to investigate, in detail, questions of cluster conformation and dynamics. These detailed studies are a continuation from our more general work on fluorene–Ar_n clusters which were described in a recent publication.²⁷

Aromatic–Ar complexes in particular have been well characterized over the years by a large number of experimental and theoretical studies. In general the argon atoms are observed to reside over the aromatic rings at a distance of approximately 3.5 Å, with displacements of position being determined by various ring substituents. The planar nature of the aromatic systems often gives rise to equivalent binding sites on opposite sides of the ring. For Ar₂ and larger complexes one question is then, are the complexes one or two sided? Using the accepted nomenclature⁶ these are represented as (2|0) and (1|1), respectively. The relative energetics of these structures are determined by a balance between the stabilizing influence of the Ar–Ar interaction and the destabilizing influence of a shift in Ar position on the aromatic system required to accommodate the second Ar. In multi-ring aromatic systems it would seem that accommodation of “one-sided” structures would be more likely.

A number of studies have identified different structural isomers in Ar_n clusters using a variety of experimental techniques.^{9,14–18,23,26,27} In the majority of cases only REMPI spectra or fluorescence excitation are available which identify multiple isomers by the appearance of distinct peaks. Spectral shift additivity rules and other spectral clues are used to determine the assignments but often the analysis is not definitive. Calculations of various types are often applied to support the isomer assignments.^{2,9,14–17,20–24} Definitive

identification of structural isomers can be made by more sophisticated experimental measurements including spectral hole burning,^{8,28,29} ionization wavelength selective resonance enhanced multiphoton ionization (REMPI) spectra^{7,8,12,15,17} and more recently zero electron kinetic energy (ZEKE) and mass analyzed threshold ionization (MATI) photoelectron spectroscopy.^{18,27,30,31}

One of the major questions in the area of molecular clusters is the relative stability of different isomers and the role they play in cluster dynamics. In answering these questions calculations have been most useful with experimental measurements providing only limited information. Molecular dynamics and Monte Carlo calculations study the cluster properties as a function of temperature and monitor phase changes, isomer interconversion, dissociation and other dynamical processes.^{9,14,23,26,32} These processes can be well monitored and characterized by the calculations but, of course, within the limits of accuracy of the potentials and methods used. Detailed experimental information on cluster dynamics is limited. Dissociation dynamics are the easiest to measure experimentally because the reactants and products are different masses and thus mass spectrometry can be applied to distinguish reactants from products. More subtle dynamics such as isomer interconversion, surface crossing, 2D–3D transitions, melting, etc. are much more difficult to measure because of the lack of sensitive probes. Dispersed fluorescence, for instance, is difficult to apply to larger clusters due to the lack of mass resolution. Careful measurement of absorption spectra linewidths, coupled with calculations, can give some insight into the onset of dynamics, but usually the dynamic processes responsible for the broadening cannot be uniquely identified. It is our goal in this study, and future work, to apply probe techniques to cluster dynamics which will allow direct measurement of specific dynamic processes. Any experimental information gained on the specifics of cluster dynamics should be useful in comparison to calculations.

In our previous study,²⁷ we have clearly identified two distinct fluorene–Ar₄ cluster isomers, assigned as (2|2) and (3|1). A key element in unambiguously identifying the two conformation was measuring distinct mass analyzed thresh-

old ionization (MATI) spectra when pumping the respective isomer S_1 origins. MATI has the advantage that it is a mass resolved technique which simultaneously has the spectral discrimination of photoelectron spectroscopy. In this way different isomers, of the same mass, can still be distinguished. As will be shown, this allows the dynamic evolution between cluster isomers to be measured.

II. EXPERIMENT

A detailed description of the experimental apparatus has been given elsewhere,²⁷ so only a brief synopsis is given here. Two color 1+1 REMPI spectroscopy with mass resolved detection is used to study the spectroscopy of the S_1 electronic state of the jet cooled clusters. Mass analyzed threshold ionization (MATI) spectroscopy,³³ the mass resolved equivalent of zero electron kinetic energy (ZEKE) spectroscopy, is used for the photoelectron spectroscopy of the ion ground state. References 27, 34, and 35 give a complete description of our application of ZEKE and MATI to the study of molecular clusters.

The nanosecond laser system employed in these experiments consists of two dye lasers (Lumonics HD-500) pumped by the second harmonics of a pulsed Nd:YAG (Continuum NY-61) operating at 20 Hz. The visible output of the each dye laser has a pulsewidth of 6 ns and a bandwidth of 0.04 cm^{-1} . Both dye lasers are frequency doubled and one functions as the pump and the other as the probe. The pump and probe lasers were temporally overlapped by appropriate optical delay and spatially overlapped in the vacuum chamber under slightly focused conditions. Care was taken to minimize any signal from either laser alone.

A pulsed supersonic beam originates in the first of two differentially pumped chamber. The nozzle has a sample container which contains the fluorene sample (Aldrich) and is heated to 100°C . This gives a fluorene vapor pressure of 1 Torr. For complexation of fluorene with Ar, a mixture of 10% Ar in He or Ar in Ne was used in the expansion. The backing pressure was varied from 1.4 to 2.5 bar in order to optimize the desired clusters. The pulsed beam is skimmed and enters the second chamber where the spectroscopy takes place.

The REMPI spectra were obtained by fixing the probe slightly higher than the ionization potential of the complex and scanning the pump. Probe energy and intensity were adjusted to avoid any dissociation from higher clusters. The MATI spectra were obtained by fixing the pump to the S_1 vibronic band of interest and scanning the probe through the IP. The MATI spectra were somewhat difficult to obtain due to the challenge of separating the prompt background ions from the Rydbergs of interest. The separation was particularly difficult due to the heavy masses of these large species and the coincidental near overlap of fluorene- Ar_4 (326 amu) and the fluorene dimer (332 amu) which was always present as a background. To achieve clean separation of the prompt and MATI signals we implemented a pulsed Wiley-McClaren³⁶ extraction scheme in which the upper grid pulsewidth was varied to act as a mass filter. In this way the contribution from the fluorene dimer could be eliminated. The MATI scheme used a delayed discrimination field of

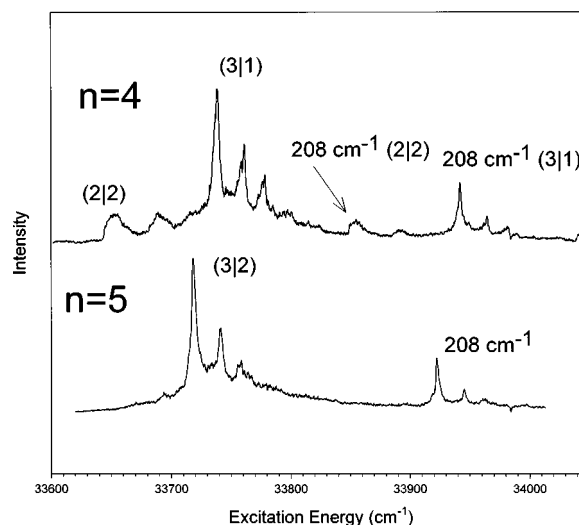


FIG. 1. Mass gated MPI spectra of the S_1 state of fluorene- Ar_n clusters with $n=4$ and 5. The spectra were obtained using two colors where the pump laser was scanned and the probe was fixed slightly above the IP so as to limit the ion internal energy to prevent ion fragmentation. The assignments of isomer bands is shown, and discussed in the text.

-2 V/cm and an extraction pulse of 560 V/cm which was delayed $\geq 15 \mu\text{s}$. The ions then traverse the TOF mass spectrometer and are detected on dual stack microchannel plates (Galileo Electro-Optic Corp.).

III. RESULTS

A. S_1 spectra

Mass resolved cluster S_1 spectra were obtained using a 1+1 two color photoionization scheme. The probe laser was tuned slightly above the cluster IP's in order to minimize the potential for cluster fragmentation in the ion. The spectra for the $n=4$ and $n=5$ clusters are shown in Fig. 1. The $n=4$ spectrum exhibits a rich structure which has been assigned to at least two isomers. The assignment of spectral features to distinct isomers, rather than vibronic structure, was unequivocally determined by MATI photoelectron spectroscopy.²⁷ The reddest peak at $33\,652 \text{ cm}^{-1}$ (compared to the fluorene monomer origin of $33\,779 \text{ cm}^{-1}$) is assigned as the (2|2) conformation based on extrapolation of the shifts from the known (1|1) cluster for which the structure is definitively known from rotationally resolved spectra.³⁷ The peak 42 cm^{-1} to the blue of this is assigned as an intermolecular vibration, again by analogy to the (1|1) cluster and from photoelectron spectra.²⁷ The largest peak at $33\,739 \text{ cm}^{-1}$ has been assigned as the origin of the (3|1) structure. While this is less definite, the assignment is consistent with the expected shifts from small clusters as well as the appearance of larger cluster shifts.

The $n=4$ spectrum also shows a small vibronic band at higher energy which is assigned as the 208 cm^{-1} band of the fluorene moiety. This band exhibits the same structure as the origin with multiple isomers present.

The $n=5$ spectrum exhibits a single isomer origin with some intermolecular vibronic bands to the blue and an overall broad background. The sharp feature is assigned to the

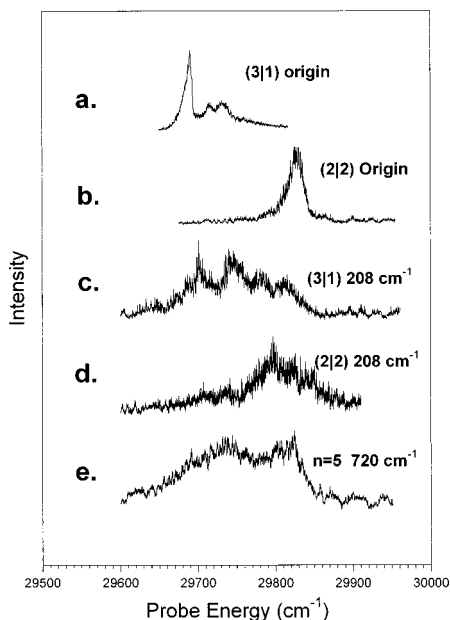


FIG. 2. MATI spectra of fluorene-Ar₄ clusters. Each spectrum was obtained by pumping either the S_1 origin or an excited vibrational band and scanning the probe in the region of the ionization potential. Spectrum (e) was obtained by pumping the $n=5$, 722 cm^{-1} band and monitoring the $n=4$ product.

origin of the (3|2) structure. This feature is red shifted from the $n=4$ (3|1) structure in a manner which is consistent with addition of an argon to a side which already has one. The broad structure could be due to thermal population in the (3|2) structure or perhaps due to other minor isomers.

B. MATI spectra

MATI spectroscopy was performed by tuning the pump laser to a particular resonance and then using the probe laser to further excite transitions to cation ground state vibrations. Figures 2(a) and 2(b) show the MATI spectra in the region of the cation origin obtained from pumping the S_1 origins of both the (3|1) and (2|2) isomers of the $n=4$ cluster, respectively. These spectra are well defined and distinct such that the two isomers can be easily distinguished by the appearance of the spectra. In experiments below these will be used as fingerprints to identify each isomer. For comparison the S_1 to cation origin transition of the fluorene monomer is at 29 962 cm^{-1} . Reference 27 has a complete summary of the transition energies.

The $n=5$ cluster is not probed directly at higher energy but rather it is excited above the dissociation threshold for loss of one Ar, thus producing an $n=4$ product which is then probed using MATI spectroscopy.

C. $n=4$ cluster dynamics

Experiments at higher energy are reported for three bands. The 208 cm^{-1} band of the (2|2) complex at 33 850 cm^{-1} , the 208 cm^{-1} band of the (3|1) complex at 33 947 cm^{-1} and the 722 cm^{-1} band of the (3|2) complex at 34 438 cm^{-1} . Previous experiments on fluorene-Ar_{*n*} $n=2$ and 3 clusters,²⁷ aniline-Ar₂,³⁸ and other similar clusters^{11,39}

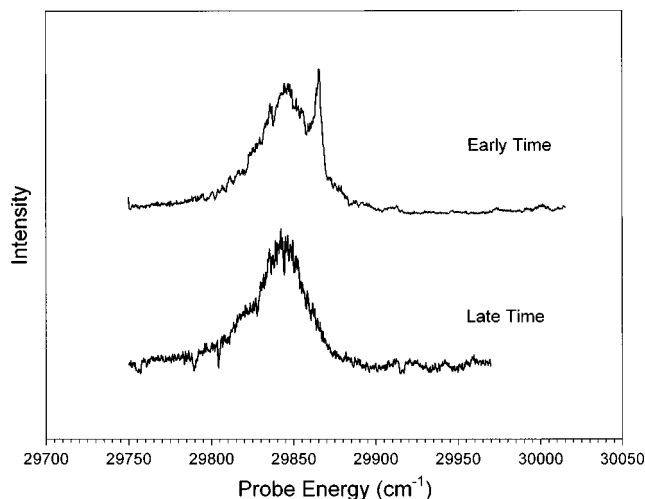


FIG. 3. Nanosecond time resolved ZEKE spectra of fluorene-Ar₃ obtained by pumping the S_1 208 cm^{-1} band. The spectra are scanned at early and late delay as indicated.

have indicated that excitation of vibronic bands above the S_1 origin lead to rapid redistribution of the energy into the intermolecular modes. This has been measured to occur in 10's to 100's of picoseconds and is shown to increase in rate with increased cluster size.²⁷ This redistribution has been observed with a number of techniques. Figure 3 demonstrates the manifestation of this redistribution in the MATI spectrum for the fluorene-Ar₃ cluster excited to 208 cm^{-1} . This spectrum was obtained with nanosecond probing at early and late time. Early time denoting direct temporal overlap of the pump and probe pulses and late time being a six nanosecond optical delay of the probe. The MATI spectrum was measured in the region of the $\Delta v=0$ transition with the sharp peak being assigned to the same vibration as the 208 cm^{-1} S_1 band which shifts to 216 cm^{-1} in the cation. The broad, red-shifted structure is assigned to the $\Delta v=0$ transitions of the intermolecular vibrational modes which have become populated by redistribution. The red shift is consistent with the observation that many of the intermolecular modes decrease in frequency in the cation. The behavior of the $n=3$, 208 cm^{-1} band is used as a model for interpreting similar structure in the $n=4$ cluster.

Figures 2(c) and 2(d) show the MATI spectrum of the (3|1) and (2|2) bands excited to 208 cm^{-1} , respectively. These spectra are probed at early time in the region of the $\Delta v=0$ transition. The signal to noise ratio is limited but the results are rigorously reproducible over a number of scans. The spectrum of the (2|2) complex is readily interpreted based on MATI spectra of smaller clusters and other cluster systems. There is a broad band which is slightly red shifted from the expected position of the $\Delta v=0$ of the 208 cm^{-1} band. This is due to rapid redistribution of vibrational energy in the S_1 state from the chromophore to the intermolecular vdW modes. The red shift is due to the decrease in vdW frequencies in the cation. The MATI spectrum of the (3|1) complex is more difficult to interpret. The structure appears broad indicating that redistribution has occurred but it is shifted to the blue of where one might expect based on ar-

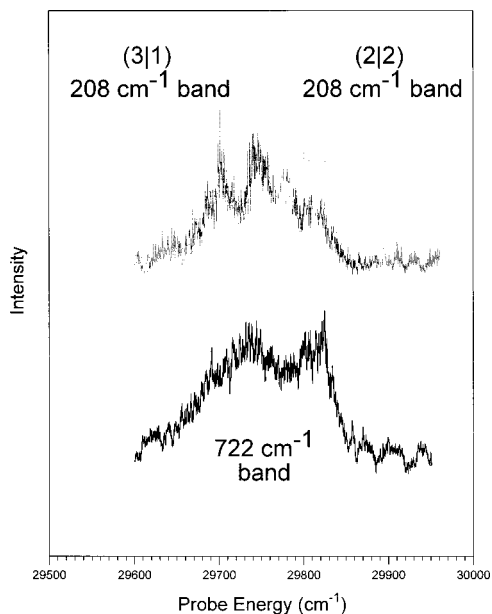


FIG. 4. Overlapped $n=4$, 208 cm^{-1} MATI and $n=5$, 722 cm^{-1} MATI. The sum of the first two discrete spectra reproduce the $n=4$ product MATI suggesting the existence of both $n=4$ isomers upon dissociation from the $n=5$ complex.

guments above for the (2|2) isomer. Although the spectrum is broad there is a well formed vibrational progression to the blue with spacings of 43, 38, and 30 cm^{-1} . This agrees quite well with the vibrational band in the MATI spectrum of the (3|1) complex from the S_1 origin, which shows a band at 42 cm^{-1} . By analogy to other clusters this can be assigned as an Ar–chromophore stretching motion. Thus, although this structure is to the blue it can be assigned as due to the (3|1) isomer.

D. $n=5$ cluster dissociation

As mentioned the $n=5$ cluster has only a single conformation. However, an interesting situation is presented in the dissociation dynamics of this cluster since there are two isomer products possible upon loss of one Ar. For this experiment the 722 cm^{-1} band of the $n=5$ cluster is excited at $34\,438\text{ cm}^{-1}$. The reaction products are probed by scanning the MATI spectrum of the $n=4$ products. Experiments on smaller clusters ($n=2,3$) have shown that dissociation from the 722 cm^{-1} band is prompt on the nanosecond time scale and only products, not reactants, are expected to be observed. By pumping the 722 cm^{-1} band, which is above the dissociation limit for $n=5$, one obtains information on the excess energy in the $n=4$ product. This will be important in analyzing the post dissociation product dynamics.

Figure 2(e) shows the MATI spectrum of the $n=4$ products when pumping the 722 cm^{-1} band of the $n=5$ complex. The product band is quite broad indicating significant vibrational energy in the intermolecular modes of the product. Most importantly the spectrum clearly shows structure due to both the (2|2) and (3|1) isomers. In fact one can reproduce the $n=4$ product MATI spectrum almost exactly by adding together the spectra of the (2|2) and (3|1) isomers as shown in Fig. 4.

TABLE I. Selected computational results.

Cluster	Isomer	Energy (kcal/mol)	Energy (cm^{-1})	Binding energy (cm^{-1})
Benzene	(0 0)	0.00	0	
Benzene–Ar	(1 0)	–1.13	–394	394
Fluorene	(0 0)	0.00	0	
Fluorene–Ar	(1 0)	–1.41	–493	493
Fluorene–Ar ₂	(1 1)	–2.84	–993	500
Fluorene–Ar ₃	(2 1)	–4.41	–1543	550
Fluorene–Ar ₄	(3 1)	–6.03	–2109	566
	(2 2)	–5.99	–2095	552
Fluorene–Ar ₅	(3 2)	–7.62	–2665	556–570

E. Calculations

We performed a series of calculations using the HyperChem⁴⁰ molecular modeling program on the fluorene–Ar_{*n*} van der Waals complex. A simple Lennard-Jones 6-12 potential is implemented to describe the nonbonded pairwise interactions present in these clusters. The values used for the atom–atom potentials parameters, σ_{ij} and ϵ_{ij} , are given in Table I of Ref. 27.

Selected single point energies of geometry optimized structures are listed in Table I. Here we see, as expected, a stabilization in the energy relative to the monomer as each argon atom is added. In addition, one can determine the binding energy for each cluster by taking the absolute difference in energy between the n cluster of interest and the $n-1$ cluster.

To determine the reliability of these calculations, our result for the binding energy of the benzene–Ar complex is compared with previous results. The binding energy of this complex is reported to be $<340\text{ cm}^{-1}$ as determined by high resolution UV spectroscopy.⁴¹ Leutwyler, Even, and Jortner calculate the energy to be 393 cm^{-1} using a similar 6-12 potential.⁴² Additionally, Schlag *et al.* report a MP2 calculation of 380 cm^{-1} .⁴³ Our calculations (Table I) predict the ground state binding energy of benzene–Ar to be 394 cm^{-1} , in direct agreement with previous results. In addition, the S_1 binding energy of fluorene–Ar has been bracketed experimentally by our group²⁷ to be $410\text{--}593\text{ cm}^{-1}$, and by others¹ to be $470\pm 95\text{ cm}^{-1}$. Again, our calculations predicting D_e at 493 cm^{-1} are in good agreement with these two ranges.

A specific quantity of interest in the fluorene–Ar_{*n*} clusters is the surface crossing energy. The two complexes of particular interest here are the fluorene–Ar complex and the fluorene–Ar₄ complex. The surface crossing energy of a single argon can be determined from the first complex, and the second will provide information on activation energy of multiple argon complexes. As a means of calculating this transition state energy several steps were taken. The first reasonable approach is to start with the single argon complex.

The fluorene molecule is aligned in a fixed axis frame with the center of mass at the origin. The long axis is aligned with the x axis, the short axis is aligned with the y axis, and the axis perpendicular to the plane of the fluorene is aligned with the z axis.

To search for the transition state minimum, a brute force

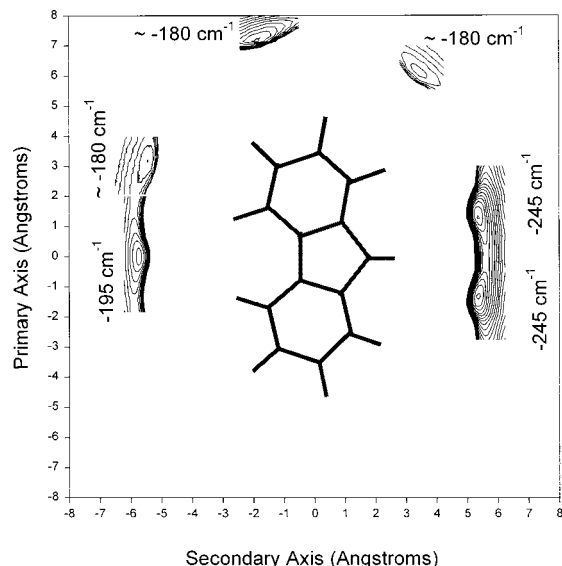


FIG. 5. Fluorene-Ar surface crossing wells obtained by collecting single point energies in a two dimensional grid search in the plane of the fluorene moiety.

grid search technique is implemented. It is practical to first study the single argon complex before moving on to the case of four or more argons. The method employed here is as follows: the argon is scanned through a three dimensional box in the area of interest. At each point in this box the single point energy of the argon is recorded as well as its coordinates. This resulting structure is then geometry optimized using a Polak-Ribiere approach. This conjugate gradient method will minimize the structure to one of its local minima depending on the starting position of the argon. Once minimized, the final energy and final coordinates of the argon are recorded.

The local minimum structures that are arrived at after each optimization are located either on the edge of the fluorene or on the top or bottom. The well depths of the edge minimum can be seen in Fig. 5. Given the planar symmetry of fluorene it is assumed that a transition state between a minimum on top (bottom) and a minimum on the edge is equivalent to a surface crossing transition state.

The resulting data from each box is then analyzed, keeping only the points that have a nearest neighbor that minimizes to a different local minimum. If this occurs between grid points then the argon has stepped over the transition barrier and a possible transition state point and energy have been bracketed. This procedure will create a line of possible transition states. By finding the minimum energy on this line one can locate the transition state. Additionally, by knowing the energy of the reactants and products one can determine the activation energy.

For the fluorene-Ar complex, the minimum transition state energy is calculated to be approximately -233 cm^{-1} (-0.66 kcal/mol) relative to the fluorene monomer. This transition state is located 5.1 \AA along the secondary axis, 1.7 \AA along the primary axis, and 1.65 \AA above the plane of the molecule, as shown in Fig. 6. Due to the symmetry of the parent, an identical transition state is located on both sides of

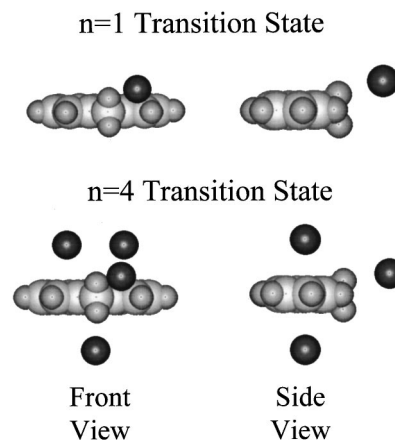


FIG. 6. Calculated transition states for the fluorene-Ar and fluorene-Ar₄ complexes.

the fluorene σ_v and σ_h planes. Table II gives the position and energy of the possible transition states. It is assumed that the lowest energy transition state is the most likely path for surface crossing. This predicts an activation energy of 260 cm^{-1} for the single argon complex. The side crossing energy represents 53% of the Ar binding energy. Schmidt *et al.*,⁴⁴ using similar atom-atom potential calculations, determined a side crossing energy of 196 cm^{-1} in benzene-Ar. However, benzene-Ar is a more weakly bound system (352 cm^{-1}) where the surface crossing is 56% of the binding energy. Surface crossing thresholds have also been determined in dynamical calculations on similar systems with reported values¹⁹ of $\sim 300\text{ cm}^{-1}$.

A similar analysis can be performed on the fluorene-Ar₄ complex. The only difference is that each time the argon is translated to a new grid point, the remaining three argons must be reoptimized to account for their effect on the fourth argon. Under this new restriction, the same procedure is followed as above. The energy of the fluorene-Ar₄ transition state is -248 cm^{-1} . In this case there is an added complication due to the fact that the forward and reverse reactions are not identical since it is the (2|2) and (3|1) structures which are connected by the surface crossing. The activation energy to the transition state depends on whether one is approaching from the (2|2) or (3|1) structure. The activation energy for the respective starting positions are calculated to be

TABLE II. Transition state positions and energies for surface crossing.

	X (\AA) ^a	Y (\AA) ^a	Z (\AA) ^a	T.S. energy (cm^{-1})	Activation energy (cm^{-1})
Fluorene-Ar	5.1	1.7	1.65	-233^b	260
	-5.8	-0.25	0	-199^b	294
	3.4	6.15	0	-184^b	310
Fluorene-Ar ₄	5.35	1.47	1.4	-248^c	315
	5.13	1.65	-1.5	-259^c	294

^aThe center-of-mass of the fluorene is at the origin.

^bRelative to monomer energy (0.00 cm^{-1}).

^cRelative to the (2|1) calculated energy (1542 cm^{-1}).

294 cm^{-1} from the (2|2) and 315 cm^{-1} from the (3|1). This is seen in Fig. 6 and noted in Table II.

IV. DISCUSSION

A. $n=4$ cluster dynamics

From the experimental data it is apparent that upon excitation to 208 cm^{-1} there is no (or very little) interconversion between the $n=4$ isomer structures. This is in spite of the fact that the energy is redistributed in the Ar motion, as evidenced by the broad and shifted MATI spectra. This lack of surface crossing was initially somewhat surprising but is supported by the above calculations and previous work. Most previous studies have used molecular dynamics simulations to probe surface crossing and other dynamic processes. This has been done by looking for evidence of surface crossing as a function of simulation temperature or energy. The evidence comes in the form of average deviations of the Ar position and/or appearance of changes in the caloric curve which might be indicative of such behavior. These calculations on similar aromatic-Ar complexes¹⁰ support the value of the barrier found in our own calculations.

B. $n=5$ dissociation dynamics

As shown above, the dissociation of the $n=5$ cluster at 722 cm^{-1} clearly produced two isomer products, the (2|2) and the (3|1). The primary question is whether the distinct isomers were produced in the dissociation via separate reaction channels, or was a single $n=4$ isomer produced which subsequently equilibrates to the two structures through a surface crossing transition. The maximum excess energy available in the product is determined, from calculations, to be $\sim 210 \text{ cm}^{-1}$, or in the range of $100 < E_{\text{excess}} < 250 \text{ cm}^{-1}$ as inferred from experimental data (see Appendix). The data from the $n=4$ cluster at 208 cm^{-1} clearly indicates that surface crossing is not taking place to any significant extent at that excess energy. In the final analysis surface crossing in the product cannot be completely ruled out though it seems unlikely based on the evidence above.

What are the dynamic considerations then for having two reaction channels for dissociation of the $n=5$ clusters? Dissociation of such clusters is considered to take place via a serial dissociation mechanism in which energy is randomized in the intermolecular Ar vibrational modes prior to dissociation. Presumably dissociation to produce the $n=4$ (2|2) structure would occur from the (3|2) reactant structure. Production of the (3|1) product could also come from the (3|2) reactant, or perhaps from a (4|1) structure produced in a rearrangement. Experimentally from Fig. 2 it is clear that both products are formed with similar propensity. The exact ratio of the two products is difficult to quantify but if we assume equal cross sections for the $\Delta v=0$ MATI transitions then the integrated area of the peaks shows that the (3|1) is the somewhat more abundant product. The product state branching ratios, in the statistical limit, depend on the relative size of the product channel phase space which in turn depends on the energetics of each channel and the vibrational modes. Based on the ground state calculations the (3|1) product is lower in energy by 15 cm^{-1} . In the excited state however,

we estimate (Appendix) that the (2|2) product is more stable by 25 cm^{-1} . Given the barrierless dissociation expected, a very loose transition state can be assumed and a phase space approach used to calculate the densities of states in the product clusters, and hence calculate the rates and branching ratios.⁴⁵ To date we have not performed such calculations. Parneix *et al.*³² have done calculations for similar conformational questions in aniline-Ar₂. They in fact observe that the density of states in the product clusters depends on the cluster structure as expected. Thus not only the energetics but the details of the product structure need to be considered in product formation. The possible role of the (4|1) reactant, produced by redistribution of the (3|2) isomer prior to dissociation, may also need to be considered. We are planning molecular dynamics simulations to probe these questions.

V. CONCLUSION

MATI spectroscopy has been shown to be a sensitive isomer specific probe in studying the molecular dynamics of medium sized clusters. A detailed study of the fluorene-Ar₄ and fluorene-Ar₅ complex has shown the existence of two isomers for Ar₄. In addition, the dissociation of the $n=5$ complex has proven to produce both of these isomers. Our calculations have shown that an excess energy of $\sim 200 \text{ cm}^{-1}$ (Appendix) is left in the Ar₄ complex. Experiments verify this prediction giving an excess energy range of 100–250 cm^{-1} in the $n=4$ product.

Calculations have shown that the energy needed for surface crossing in the $n=4$ complex is 315 cm^{-1} . This activation energy is above the excess energy contained in the $n=4$ product, suggesting that no surface crossing occurs after dissociation of $n=5$ complex.

With these conclusions, one is led to believe that dissociation of the $n=5$ complex has two reaction channels. One is dissociation of an argon from the $n=3$ side of the cluster, and the other is dissociation from the $n=2$ side. This observation is supported by a calculated energy of dissociation difference of only 14 cm^{-1} between the two reaction channels.

ACKNOWLEDGMENT

We gratefully acknowledge the NSF for financial support of this project under Grant No. CHE-9523575.

APPENDIX

The following outlines the calculation of the maximum excess energy available in the $n=4$ product after dissociation of the $n=5$ cluster. From calculations, the ground state binding energy of the 5th Ar is 556 or 570 cm^{-1} depending on whether the product is (3|1) or (2|2), respectively. The excited state binding energy is different than the ground state binding energy but not in an obvious way. For the $n=1$ complex the -40 cm^{-1} spectral shift gives directly the increase in total cluster binding energy. However, for $n=5$ the shift is $\sim -80 \text{ cm}^{-1}$ but it is not clear how to apportion this to the different argons. From analysis of smaller cluster spectral shifts it would appear that the side with two argons have a 40 cm^{-1} stabilization for each Ar whereas the side with

three-argons contributes essentially no stabilization. Since we are interested in the lower limit of the binding energy (i.e., maximum energy in the dissociation products) we will assume it is the ground state calculated value. The zero point energy also needs to be considered. This is roughly 40 cm^{-1} and again reduces the calculated binding energy. Thus we have a calculated binding energy range of $516\text{--}530\text{ cm}^{-1}$. Given an excitation to the 722 cm^{-1} band this leaves the maximum product energy of $\sim 200\text{ cm}^{-1}$.

- ¹D. H. Levy, *Adv. Chem. Phys.* **47**, 3742 (1981).
- ²M. J. Ondrechen, Z. Berkovitch-Yellin, and J. Jortner, *J. Am. Chem. Soc.* **103**, 6586 (1981).
- ³U. Even, A. Amirav, S. Leutwyler, M. J. Ondrechen, Z. Berkovitch-Yellin, and J. Jortner, *Faraday Discuss. Chem. Soc.* **73**, 153 (1982).
- ⁴S. Leutwyler, U. Even, and J. Jortner, *J. Chem. Phys.* **79**, 5769 (1983).
- ⁵K. Butz, D. L. Catlett Jr., G. E. Ewing, D. Krajnovich, and C. S. Parmenter, *J. Chem. Phys.* **90**, 3533 (1986).
- ⁶N. Mikami, Y. Sugahara, and M. Ito, *J. Phys. Chem.* **90**, 2080 (1986).
- ⁷T. Troxler, R. Knochenmuss, and S. Leutwyler, *Chem. Phys. Lett.* **159**, 554 (1989).
- ⁸R. Knochenmuss and S. Leutwyler, *J. Chem. Phys.* **92**, 4686 (1990).
- ⁹S. Leutwyler and J. Bosiger, *Chem. Rev.* **90**, 489 (1990); J. Bosiger, R. Bombach, and S. Leutwyler, *J. Chem. Phys.* **94**, 5098 (1991).
- ¹⁰E. R. Bernstein, in *Studies in Physical and Theoretical Chemistry*, edited by E. R. Bernstein (Elsevier, Amsterdam, 1990), Vol. 68, p. 551.
- ¹¹A. Heikal, L. Banares, D. H. Semmes, and A. H. Zewail, *Chem. Phys.* **157**, 231 (1991).
- ¹²T. Troxler and S. Leutwyler, *J. Chem. Phys.* **95**, 4010 (1991).
- ¹³E. A. Outhouse, G. A. Bickel, D. R. Demmer, and S. C. Wallace, *J. Chem. Phys.* **95**, 6261 (1991).
- ¹⁴N. Ben-Horin, U. Even, and J. Jortner, *J. Chem. Phys.* **97**, 5988 (1992); N. Ben-Horin, D. Bahatt, U. Even, and J. Jortner, *ibid.* **97**, 6011 (1992).
- ¹⁵M. Schmidt, M. Mons, and J. Le Calve, *J. Chem. Phys.* **96**, 2404 (1992).
- ¹⁶C. Guillaume, M. Mons, J. Le Calve, and I. Dimicoli, *J. Phys. Chem.* **97**, 5193 (1993).
- ¹⁷N. Ben-Horin, U. Even, J. Jortner, and S. Leutwyler, *J. Chem. Phys.* **97**, 5296 (1992).
- ¹⁸M. C. R. Cockett, K. Okuyama, and K. Kimura, *J. Chem. Phys.* **97**, 4674 (1992).
- ¹⁹P. Hermine, P. Parneix, B. Coutant, F. G. Amar, and Ph. Brechignac, *Z. Phys. D* **22**, 529 (1992).
- ²⁰P. Parneix, F. G. Amar, and Ph. Brechignac, *Z. Phys. D* **26**, 217 (1993).
- ²¹T. Troxler and S. Leutwyler, *J. Chem. Phys.* **99**, 4363 (1993).
- ²²A. Penner and A. Amirav, *J. Chem. Phys.* **99**, 9616 (1993).
- ²³D. Bahatt, A. Heidenreich, N. Ben-Horin, U. Even, and J. Jortner, *J. Chem. Phys.* **100**, 6290 (1994); A. Heidenreich, D. Bahatt, N. Ben-Horin, U. Even, and J. Jortner, *ibid.* **100**, 6300 (1994).
- ²⁴R. Knochenmuss, D. Ray, and W. P. Hess, *J. Chem. Phys.* **100**, 44 (1994).
- ²⁵R. Sussman, U. Zitt, and H. J. Neusser, *J. Chem. Phys.* **101**, 9257 (1994).
- ²⁶E. Shalev, N. Ben-Horin, U. Even, and J. Jortner, *J. Chem. Phys.* **95**, 3147 (1991).
- ²⁷Xu Zhang, Jonathan Pitts, Ravindrakumar Nadarajah, and J. L. Knee, *J. Chem. Phys.* **107**, 8239 (1997).
- ²⁸E. A. Mangle and M. R. Topp, *J. Phys. Chem.* **90**, 802 (1986); R. Jefferson Babbitt and M. R. Topp, *Chem. Phys. Lett.* **127**, 111 (1986); S. A. Wittmeyer, A. J. Kaziska, A. L. Motyka, and M. R. Topp, *ibid.* **154**, 1 (1989).
- ²⁹J. M. Smith and J. L. Knee, *J. Chem. Phys.* **99**, 38 (1993).
- ³⁰M. C. R. Cockett and K. Kimura, *J. Chem. Phys.* **100**, 3429 (1994).
- ³¹For a review of the application of ZEKE spectroscopy to clusters see, K. Muller-Dethlefs, O. Dopfer, and T. G. Wright, *Chem. Rev.* **94**, 1845 (1994).
- ³²Pascal Parneix, Philippe Bréchignac, and Francois G. Amar, *J. Chem. Phys.* **104**, 983 (1996).
- ³³L. Zhu and P. M. Johnson, *J. Chem. Phys.* **94**, 5769 (1991).
- ³⁴Xu Zhang and J. L. Knee, *Faraday Discuss.* **97**, 299 (1994).
- ³⁵*Femtosecond Chemistry*, edited by Jörn Manz and Ludger Wöste (VCH, Weinheim, 1995), Chap. 4.
- ³⁶W. C. Wiley and I. H. McLaren, *Rev. Sci. Instrum.* **26**, 1150 (1955).
- ³⁷R. Sussmann, U. Zitt, and H. J. Neusser, *J. Chem. Phys.* **101**, 9257 (1994).
- ³⁸X. Zhang, J. M. Smith, and J. L. Knee, *J. Chem. Phys.* **97**, 2843 (1992).
- ³⁹D. L. Osborn, J. C. Alfano, N. van Dantzig, and D. H. Levy, *J. Chem. Phys.* **97**, 2276 (1992); J. C. Alfano, S. J. Martinez III, and D. H. Levy, *ibid.* **96**, 2533 (1992).
- ⁴⁰Hypercube, Waterloo, Ontario, Canada.
- ⁴¹H. J. Neusser and H. Krause, *Chem. Rev.* **94**, 1829 (1994).
- ⁴²Joshua Jortner, Uzi Even, Samuel Leutwyler, and Ziva Berkovitch-Yellin, *J. Chem. Phys.* **78**, 309 (1983).
- ⁴³P. Hobza, Ota Bludský, H. L. Selzle, and E. Schlag, *J. Chem. Phys.* **97**, 335 (1992).
- ⁴⁴M. Schmidt, J. Le Calve, and M. Mons, *J. Chem. Phys.* **98**, 6102 (1992).
- ⁴⁵T. Baer and W. L. Hase, *Unimolecular Reaction Dynamics: Theory and Experiment* (Oxford University Press, New York, 1996).